International Journal of Chronic Obstructive Pulmonary Disease Dovepress
open access to scientific and medical research

Open Access Full Text Article ORIGINAL RESEARCH

Abhd2, a Candidate Gene Regulating Airway Remodeling in COPD via TGF-β

Mei-Yu Lv[1,2], Ling-Ling Jin[2,3], Xi-Qiao Sang[2], Wen-Chao Shi[2], Li-Xia Qiang[2], Qing-Yan Lin[4], Shou-De Jin[2]

[1]Department of Respiratory Medicine, Harbin Medical University Cancer Hospital, Harbin, 150001, People's Republic of China; [2]Department of Respiratory Medicine, the Fourth Affiliated Hospital of Harbin Medical University, Harbin, 150001, People's Republic of China; [3]Department of Critical Care medicine, the Second Affiliated Hospital of Xi 'an Jiaotong University, Xi'an, Shaanxi, China; [4]Department of Respiratory Medicine, Heilongjiang Provincial Hospital, Harbin, 150001, People's Republic of China

Correspondence: Shou-De Jin, Department of Respiratory Medicine, The Fourth Affiliated Hospital of Harbin Medical University, No. 37 Yiyuan Street, Nangang District, Harbin, 150001, People's Republic of China, Tel/Fax +86 0451-85939123, Email jinshoude@163.com

Purpose: The typical characteristic of COPD is airway remodeling, affected by environmental and genetic factors. However, genetic studies on COPD have been limited. Currently, the Abhd2 gene is found to play a critical role in maintaining alveolar architecture and stability. The research aims to investigate the predictive value of Abhd2 for airway remodeling in COPD and its effect on TGF-β regulation.

Methods: In humans, Abhd2 protein was obtained from peripheral blood monocytes. Peripheral blood TGF-β, pulmonary surfactant proteins (SPs), metalloproteinases, inflammatory indicators (WBC, NEU, NLR, EOS, CRP, PCT, D-Dimer), chest CT (airway diameter and airway wall thickness), pulmonary function, and blood gas analysis were used to assess airway remodeling. In animals, Abhd2 deficient mice ($Abhd2^{Gt/Gt}$) using gene trapping and C57BL6 mice were injected intraperitoneally with CSE to construct COPD models. HE staining, Masson staining and immunohistochemistry were used to observe the pathological changes of airway in mice, and RT-PCR, WB, ELISA and immunofluorescence were used to detect the expression of secreted proteins and EMT markers.

Results: COPD patients with worse pulmonary function and higher airway remodeling-related inflammatory factors had lower Abhd2 protein expression. Moreover, indicators followed the same trend for COPD patients grouped by prognosis (Group A vs Group B). Serum TGF-β was negatively correlated with Abhd2 protein expression, FEV1/FVC, FEV1, and FEV1% PRED. In mice, *Abhd2* depletion promoted deposition of TGF-β, leading to more pronounced emphysema, airway thickening, increased alveolar macrophage infiltration, decreased AECII number and SPs, and EMT phenomenon.

Conclusion: Downregulation of *Abhd2* can promote airway remodeling in COPD by modulating repair after injury and EMT via TGF-β. This study suggests that *Abhd2* may serve as a biomarker for assessing airway remodeling and guiding prognosis in COPD.

Keywords: alpha/beta hydrolase 2, COPD, TGF-β, airway remodeling, EMT

Introduction

Chronic obstructive pulmonary disease (COPD) is the leading cause of disability and even death worldwide, especially in cold regions of northern China.[1] The typical pathological features of COPD are chronic inflammation and airway remodeling, which are influenced by both genetic and environmental factors. In the process of airway remodeling, airway and lung stimulated by external factors such as pathogens and smoke may present with epithelial barrier damage, airway mucosal hyperplasia, epithelial to mesenchymal transition (EMT), smooth muscle thickening, increased basement membrane thickness, mucus hypersecretion, excessive deposition of connective tissue, alveolar elastic fiber breakage, accompanied by inflammatory cell infiltration, ultimately leading to airway structure and function changes. Repeated stimulation of airway mucosa by inflammatory factors causes sustained tissue damage and incomplete repair, culminating in airway remodeling and emphysema. However, current diagnostic and therapeutic measures are limited. Therefore, a deeper understanding of the mechanism of key factors in airway remodeling in the pathogenesis of COPD is needed.

Received: 10 October 2023
Accepted: 26 December 2023
Published: 5 January 2024

TGF-β, considered a multifunctional cytokine, has been reported by many scholars at home and abroad to be involved in the pathogenesis of airway remodeling in COPD, especially the EMT process mediated through the SMAD pathway, resulting in airway airflow limitation.[2,3] Recent studies have shown that TGF-β interacts with the expression of pulmonary surfactant proteins (SPs) and metalloproteinases, participating in multiple links such as repeated repair after alveolar tissue injury, EMT, immune defense, inflammatory mechanisms, and lipid metabolism in COPD. For example, it has been found that surfactant protein A (SP-A) or D (SP-D) gene deletion may be involved in fibrocyte activation and collagen production by regulating TGF-β.[4–7] In turn, TGF-β can competitively bind SMAD3 to inhibit SPs expression, thereby promoting pulmonary fibrosis, collagen and smooth muscle abnormal distribution.[8–10] Yang et al found that TGF-β in brain astrocytes can participate in the process of central nervous system tissue remodeling by regulating the secretion of MMP-9.[11] However, studies on upstream gene mechanisms are still limited. Interestingly, recent studies have found that cDNA cloned from cDNA libraries of emphysematous mice and encoding Alpha/beta hydrolase domain 2 (Abhd2) protein may be related to airway remodeling via TGF-β.

Abhd2, a member of the alpha/beta hydrolase superfamily, was previously known as lung alpha/beta hydrolase 2 (Labh2) and is highly expressed in the lung, adrenal, and brain tissues of mice.[12] The Abhd family contains at least 19 proteins that have recently been implicated as novel regulators of signaling in lipid metabolism because of their conserved motifs. Human Abhd2 is a 48 KD protein, which is mainly studied in hepatitis B virus reproduction, atherosclerosis and reproductive function regulation, but its biological function remains unclear.[13] In 2005, Jin et al first identified *Abhd2* expression on alveolar type II epithelial cells (AECII) and macrophages when studying the genetics of emphysema.[14] In clinical studies, Jin's team found that the rs12442260 polymorphism in the *Abhd2* is strongly associated with the risk of COPD, but further studies have not been achieved.[15] At the animal level, *Abhd2* deficient mice at 6 months of age spontaneously develop an age-related emphysematous phenotype, accompanied by airway metaplasia, mucus hypersecretion, increased macrophage infiltration, and disturbed pulmonary surfactant expression, which closely resembles the pathogenesis of emphysema in humans.[14] Therefore, *Abhd2* may be a susceptibility gene for COPD. Combined with the function of TGF-β and our previous findings of increased TGF-β expression in the lungs of *Abhd2* deficient mice, we speculated that *Abhd2* may regulate alveolar structure repair and EMT through TGF-β to participate in the pathogenesis of airway remodeling in COPD.

Based on the above, we analyzed clinical COPD patients and COPD model mice modeled to mimic human disease by smoking, which included gene trap mice ($Abhd2^{Gt/Gt}$) with a genetic background of COPD and normal mice (C57BL6). The aim of this study was to investigate (1) Abhd2 and TGF-β expression levels in the human body, and their relationship with airway remodeling and the prognosis of COPD by combining imaging, pulmonary function, and inflammatory indicators, (2) the effect of $Abhd2^{Gt/Gt}$ on the structure and secretion of airway and alveoli in COPD mice induced by CSE combined with LPS, and (3) the regulatory mechanism of *Abhd2* on airway remodeling.

Materials and Methods

Human Groups

All clinical data conformed to the Declaration of Helsinki and were collected at the Fourth Affiliated Hospital of Harbin Medical University from April 2019 to June 2022, and were approved by the Ethics Committee. Participants included 89 patients with acute exacerbation of COPD who met GOLD[16] guideline criteria (COPD) and 30 healthy controls (Health) (Figure 1). Participants with the following conditions were excluded: (1) asthma, endobronchial tuberculosis, tumor, or other diseases causing airway wall thickening; (2) primary cardiovascular and cerebrovascular diseases. For the COPD group, patients were further divided into two groups according to prognosis, Group A (general prognosis) and Group B (poor prognosis), in which Group B met any of the following: (1) pulmonary function grade above severe (stage III and IV); (2) number of hospitalizations ≥ 2 times/year; (3) mMRC ≥ 4 points.

Clinical Information

Human basic information including age, gender, weight, smoking status, pulmonary function, dyspnea scores (mMRC and CAT), blood routine, chest CT, etc. was included in the analysis. Airway mucosal remodeling was assessed by observing the tracheal transverse diameter (TD), tracheal anteroposterior diameter (AD), tracheal wall thickness (TWT), and bronchial wall thickness (BWT) in chest CT. Airway measurement was performed 10 mm above (trachea) or below (right main bronchus, RMB) the tracheal carina using IMPAX Client software.

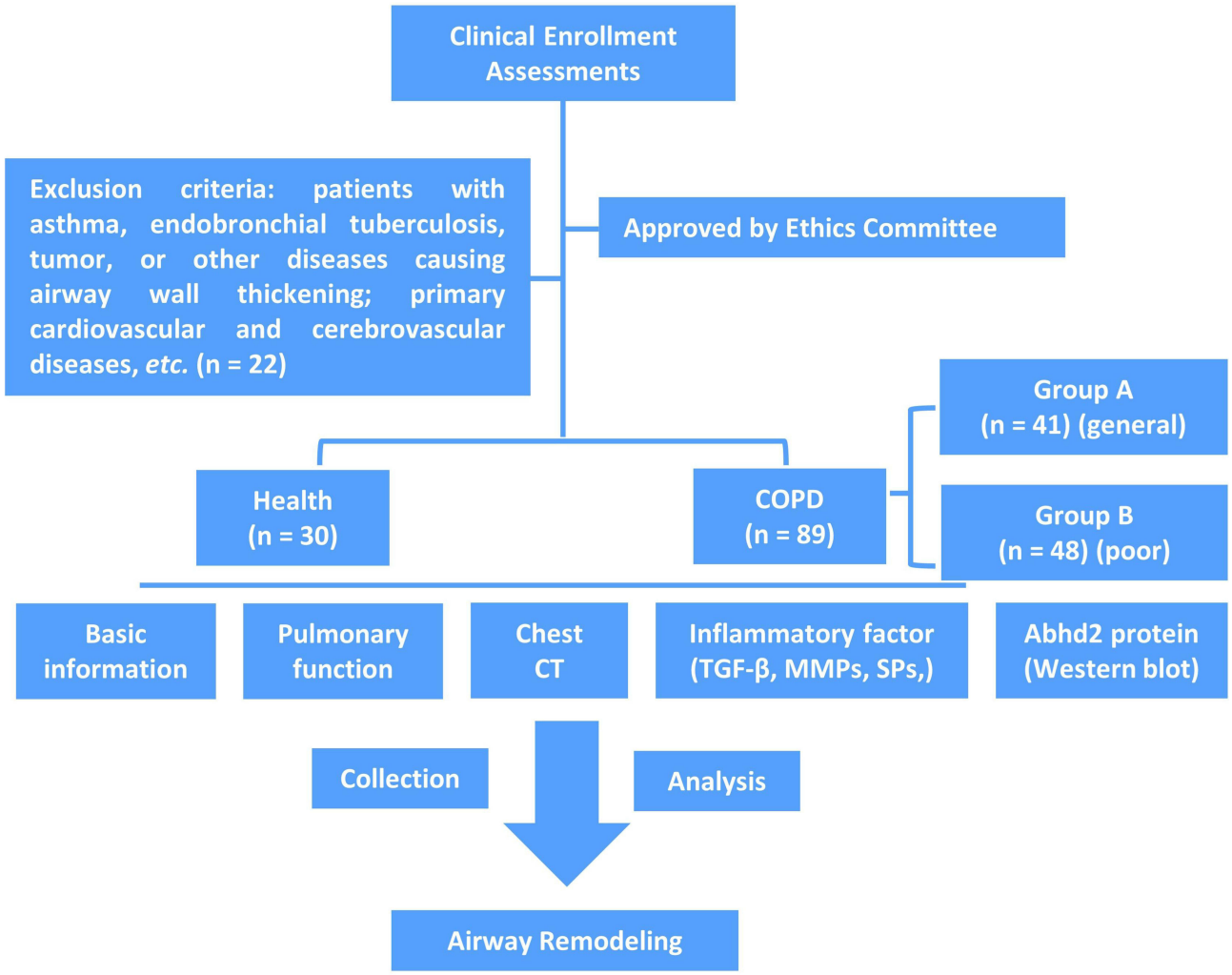

Figure 1 Flow Chart of Clinical Study.

Human Inflammatory Factor Assay

Serum was separated from peripheral blood of healthy individuals or COPD patients within 24 hours of hospitalization. Collection of bronchoalveolar lavage fluid (BALF) was achieved by bronchoalveolar lavage with warm saline by a professional physician operating bronchoscope with a negative pressure of 100 mmHg. Supernatants were obtained by centrifugation in a centrifuge at 2500 rpm at 4°C after 20 minutes of rest at room temperature and stored at −80°C until use. TGF-β (SEA124Hu, Cloud-Clone Corp.) in serum and BALF, SP-A, SP-D (Jianglai Bio, China), MMP-2, MMP-9, and MMP-12 (MLbio, China) in blood were detected using the ELISA method. The steps of reagent addition, incubation, washing, color development and termination were completed according to the instructions, and the final determination was completed with a microplate reader (Bio Tek Instrument, USA) at a wavelength of 450 nm.

Monocyte Isolation and Abhd2 Protein Assay

Monocytes were isolated from peripheral blood of COPD patients and controls. Protein extracts and protease inhibitors were prepared according to the number of samples, and the extraction of total monocyte protein was completed according to the kit instructions (Bestbio, China). The purified protein was assayed for concentration using the BCA method followed by protein separation and Western blot (WB) using SDS-PAGE in the same manner as described below. Anti-Abhd2 (1:1000 dilution, ab230417, Abcam) primary antibody was purchased from Abcam and GAPDH was used as control.

Experimental Animal

Mice used in this study were housed in SPF clean grade environments (females, 4–5 months old, weighing 16 g - 25 g). Wild type mice (C57BL6) were purchased from the Experimental Center of Peking University. *Abhd2*$^{Gt/Gt}$ mice, were obtained by gene capture technology at the Animal Experimental Center of Kumamoto University, was constructed as described previously.[14,15] All animal experiments complied with the policies of the Chinese Association of Laboratory Animal Science and were approved by the Ethics Committee of the Fourth Affiliated Hospital of Harbin Medical University.

Abhd2$^{Gt/Gt}$ mice gene identification steps were listed. (1) Genotyping of mice: The samples were taken from mouse ears and the genomic DNA was extracted by alkaline lysis, followed by PCR amplification and agarose electrophoresis. The detailed sequence of specific primers and PCR reaction systems were the same as before.[14] Gene expression results from wild-type and *Abhd2*$^{Gt/Gt}$ mice were confirmed with primer set G1-G2 and primer set G2-G3. (2) RNA analysis: RNA expression was assessed by RT-PCR. (3) Protein determination: WB method was used.

Animal Treatment

Animals were divided into the following 5 groups: (1) wild-type group (WT); (2) wild-type + CSE group (WTSM); (3) *Abhd2*$^{Gt/Gt}$ group (AB); (4) *Abhd2*$^{Gt/Gt}$ + CSE group (ABSM); (5) *Abhd2*$^{Gt/Gt}$ + CSE +SB-431542 group (ABSMSB). All mice in the labeled "SM" group received an intraperitoneal injection (i.p.) of cigarette smoke extract (CSE, 0.3 mL/20g) on days 0, 11, 22, 33, and 44, combined with airway instillation of LPS (1mg/kg) on day 14 to construct COPD model, while other groups were treated with the same amount of PBS. Mice in the ABSMSB group were administered (i.p.) with SB-431542 (10mg/kg; ab120163, Abcam) 2 hours before CSE.[17,18] Mice sacrificed and specimens collected on Day 51.

Cigarette extraction system: Five de-filtered cigarettes containing 0.8 mg nicotine, 8 mg tar, and 10 mg carbon monoxide were burned in a super clean bench, and the smoke was aspirated by a negative pressure pump (−0.1 Kpa) to dissolve it in 20 mL PBS through a three-way tube. The obtained suspension was adjusted to pH (Ph 7.2–7.4) with 0.1 mol/L NaOH and sterilized by microporous filter membrane (0.22 μm) filtration to obtain the stock solution, which was prepared immediately before use.

Collection of Pulmonary Surfactant Proteins in Mice

After anesthesia, orbital blood sampling for ELISA was performed by capillary tube in mice. Then, mice were dorsally fixed to separate the trachea and lungs as a whole. Place one end of the ophthalmic forceps between the trachea and esophagus to ensure tracheal distraction, and cut an incision of approximately 2 mm at the 3–5 tracheal cartilage rings. Lift a small amount of tracheal wall with ophthalmic curved forceps while inserting the trachea with a homemade syringe with plastic hose at the front. Subsequently, 1 mL PBS was slowly perfused and BAL was aspirated while massaging the lungs of mice after 30 s of stay to ensure a recovery rate of more than 80%. After centrifugation, the supernatant was taken to determine the expression of SP-A (SEA890Mu, Cloud-Clone Corp.), SP-C (SEB623Mu, Cloud-Clone Corp.) and SP-D (SEB039Mu, Cloud-Clone Corp.). SPs extracted from blood and BAL were stored as above and tested 3 times per sample.

Pathologic Staining

The thorax of mice was fully exposed, and the left lung was washed with PBS and stored in liquid nitrogen for RT-PCR and WB. The right lung was fixed with 4% paraformaldehyde by intratracheal instillation and extratracheal immersion, followed by routine paraffin-embedded sections (4 μm thickness) for pathological observation, including HE staining, Masson staining and immunohistochemistry. HE staining was used to observe the structural integrity of airway wall and alveoli, inflammatory cell infiltration, and smooth muscle hyperplasia in mice to evaluate airway remodeling and emphysema. Alveolar destruction was assessed by calculating MLI as previously described.[19] Pulmonary collagen fibril deposition was measured by calculating collagen volume ratio using ImageJ software. Immunohistochemistry was used to assess alveolar secretory function and structural damage, and TGF-β expression.[20] Sections were incubated for anti-TGF-β antibody (GB11179, Servicebio), anti-SP-A antibody (ab11579233011, Abcam), anti-SP-D antibody (ab220422, Abcam), anti-ProSP-C antibody (ab211326, Abcam), anti-F4/80 antibody (GB11027, Servicebio). Staining grades were determined by analyzing the number of positive cells and staining intensity using IHC Profiler and scores greater than or equal to 1 were scored as positive. Numbers of macrophage and AECII were counted using IHC ToolBox.

Real-Time PCR Analysis

Total RNA of mice was extracted by Trizol lysis method for the detection of inflammatory factors in lung tissue. Subsequently, RNA was quantified by measuring the A_{260}/A_{280} ratio with a NanoDrop spectrophotometer after completion of accumulation, washing and dissolution, and stored at −20°C. cDNA was prepared by reverse transcription of 1 μg RNA (ReverTra Ace qPCR RT Kit, Toyobo), followed by addition of FastStart ™ Universal SYBR ® Green premix (Rox) for 40 cycles (15s at 95°C;60 s at 60°C) on a real-time quantitative PCR instrument (Bio-Rad) to complete PCR amplification and analysis. Specific primer sequences were listed in Table S1 and relative mRNA expression was calculated by the $2^{-\Delta\Delta Ct}$ method.[21] All primers including GAPDH as internal reference were synthesized by Invitrogen.

Immunofluorescence Staining and Western Blotting

Paraffin sections were deparaffinized, antigen retrieval, BSA blocked and incubated overnight at 4°C for primary antibodies, such as anti-E-cadherin antibody (GB12082, Servicebio), anti-ZO1 antibody (GB111402, Servicebio) and anti-Vimentin antibody (GB111308, Servicebio), similar to immunohistochemical steps. After washing, targeted recognition was performed with incubated Cy3-labeled secondary antibodies (1:300 dilution, GB21401, Servicebio; 1:300 dilution, GB21303, Servicebio), nuclei were stained with DAPI dye, and finally fluorescence intensity was observed under a fluorescence microscope.

Lung tissue from mice was ground to powder with liquid nitrogen, and then RIPA lysate, PMSF, protease inhibitor and phosphatase inhibitor were added into EP tube. Following mixing, lysis was performed on ice for 30 min, accompanied by electrokinetic homogenate every 10 min until complete lysis. The EP tubes were centrifuged at 12,000 rpm/min for 20 min at 4 °C, and the supernatants were assayed for protein concentration using a BCA kit and stored at −80 °C after denaturation. Next, 50 μg of protein was added to 8% to 12% SDS-PAGE, and the gel was polymerized at 80 V for 30 min, followed by separation at 120 V for 1 h – 3 h until electrophoresis was stopped when bromophenol blue reached the bottom. Immediately afterwards, the proteins were transferred to PVDF membranes, followed by blocking with 5% nonfat dry milk, incubation of antibodies, color development, and machine photography (Biorad ChemiDoc XRS+, USA). Membranes were incubated with primary antibodies (SP-A, ab115791, Abcam; ProSP-C, ab211326, Abcam; SP-D, ab220422, Abcam; E-ca, ab212059, Abcam; ZO1, ab276131, Abcam; Vimentin, ab92547, Abcam; TGF-β, ab215715, Abcam; Abhd2, ab230417, Abcam; GAPDH, K200057M, Solarbio) overnight at 4 °C and secondary antibodies (GB23301, Servicebio; GB23303, Servicebio) for 2 h at room temperature.

Statistical Analysis

Results were analyzed with SPSS Statistics v.25 (SPSS, Inc.), ImageJ 1.53e (ImageJ software, USA), and GraphPad Prism 8.0.1 (GraphPad Software, LLC) and presented as mean ± SD or median or percentage. Qualitative data including age and immunohistochemical sections were assessed by Chi-square test. Significance between two groups were compared using *t*-test or Mann–Whitney *U*-test. Differences among multiple groups in animal experiments were analyzed by ANOVA analysis and post hoc multiple comparisons were performed by Bonferroni method. $P < 0.05$ was considered statistically significant.

Result

Basic Clinical Characteristics

All clinical information, including personal characteristics (age, gender, BMI, smoking), pulmonary function parameters (FEV1/FVC, FEV1, and FEV1% PRED), blood gas analysis (PaCO2 and PaO2) and dyspnea scores (mMRC and CAT) were recorded or calculated from the hospital database. The basic characteristics of COPD group and healthy people had no significant difference in statistics, which was shown in Table 1. In the COPD group, the age, smoking index, PaO2, mMRC, and CAT scores of patients in Group B with worse prognosis were higher than those in Group A ($P < 0.05$).

Evaluation of Airway Remodeling in Humans

Pulmonary function parameters revealed small airway disease in COPD (Table 1). FEV1/FVC (%), FEV1 (L), and FEV1% pred (%) were used to compare the degree of small airway airflow limitation between COPD patients and controls. In COPD patients,

Table 1 Clinical Basic Information

Groups		Overall (n = 119)	COPD (n = 89)	Control (n = 30)	Difference (95% CI)	χ2 /Z/ T	P Value
Gender, % (n)	Female	49.60 (59)	48.30 (43)	53.30 (16)	5.00 (−16.00, 26.00)	0.226	0.634
	Male	50.40 (60)	51.70 (46)	46.70 (14)			
Age (Years)		62.62 ± 9.37	63.47 ± 9.92	60.10 ± 7.05	3.37 (−0.51, 7.26)	1.719	0.088
BMI		21.89 ± 2.39	22.12 ± 2.51	21.19 ± 1.83	0.93 (−0.05, 1.92)	1.874	0.063
Smoking index		300 (0,800)	240 (0, 800)	300.00 (0, 800)	0 (0, 150)	−0.679	0.497
Post-bronchodilator pulmonary function	FEV1/FVC (%)	65.50 (55.94, 80.93)	60.17 (55.05, 66.53)	83.95 (80.39, 86.77)	22.58 (19.77, 25.87)	−8.170	**<0.001**
	FEV1 (L)	1.54 (1.12, 2.01)	1.25 (1.00, 1.56)	1.86 (1.67, 2.41)	0.68 (0.51, 0.86)	−5.909	**<0.001**
	FEV1% pred (%)	63.50 (45.13, 84.30)	49.00 (39.40, 69.45)	85.61 (83.53, 89.37)	35.90 (27.78, 42.33)	−6.855	**<0.001**

Note: Data presented as mean ± standard deviation (SD), median (P25, P75) and percentage (%). Bold font indicated emphasis. A value of $P < 0.05$ was considered statistically significant.

FEV1/FVC (%) below 70% indicated obstructive ventilatory dysfunction, and decreased FEV1 or FEV1% predicted airflow limitation that may be caused by airway spasm or remodeling ($P < 0.05$).

Chest CT showed structural changes in large airways in COPD (Figure 2, Table S2). Compared with the control group, the anteroposterior diameter of the chest increased, the airway lumen showed deformation or collapse, and some sputum remained in COPD patients (Figure 2A and B). Moreover, the thickness of tracheal wall (TWT) and bronchial wall (BWT) in COPD group

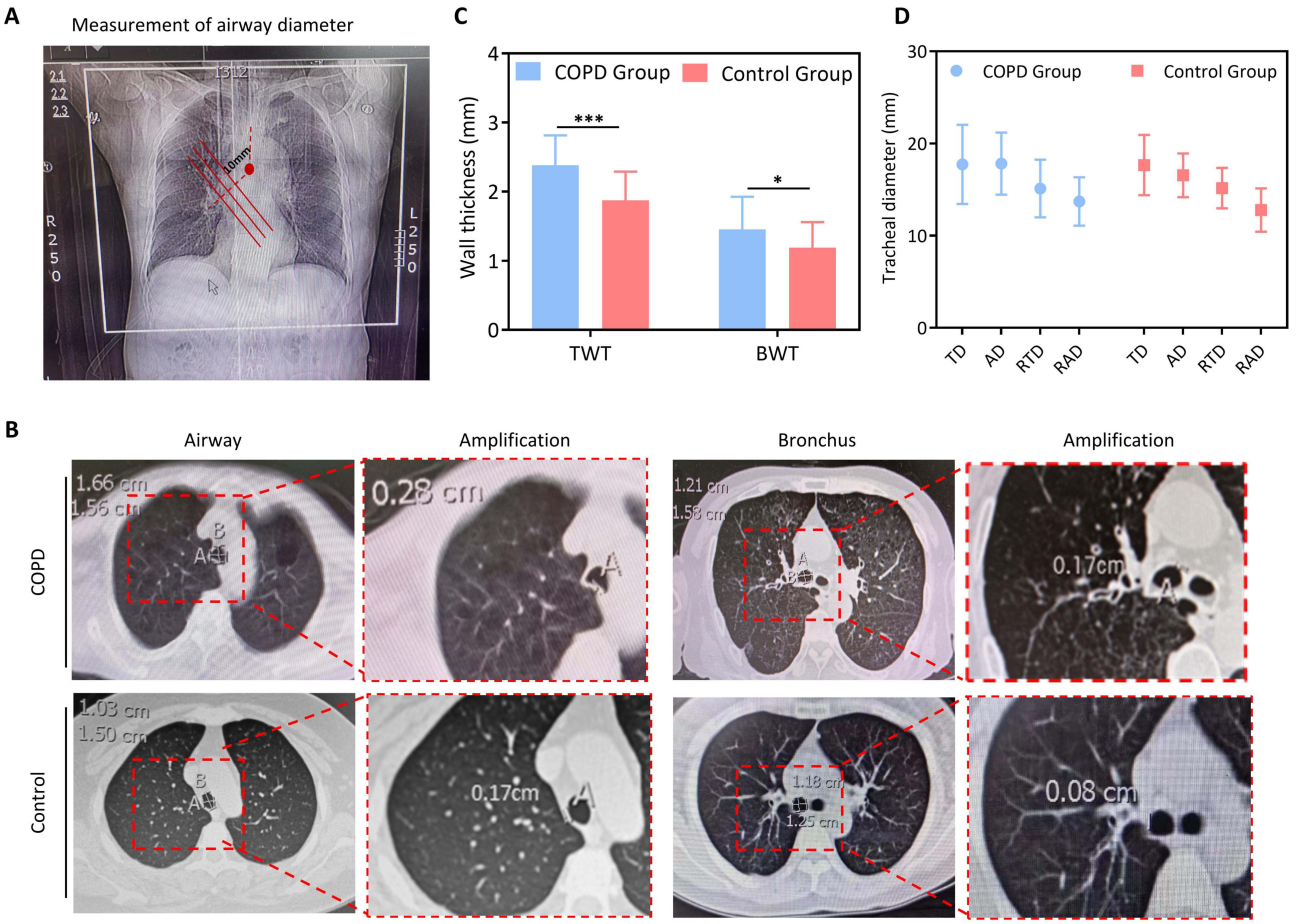

Figure 2 Clinical lung imaging changes in COPD. (**A**) Graphical representation of airway measurements in coronal chest CT. (**B**) Measurement of trachea and bronchus in horizontal chest CT. (**C**) Increased thickness of airway wall and bronchial wall on chest CT in COPD. (**D**) Diameter of trachea and right main bronchus between groups. *$P < 0.05$, ***$P < 0.001$.

increased significantly by measuring the airway diameter (Figure 2C) ($P < 0.05$). However, there was no significant difference in transverse and anteroposterior airway diameters (TD, RTD, AD, RAD) between the two groups (Figure 2D) ($P > 0.05$).

Inflammatory markers in peripheral blood and BALF reflected the state of airway inflammation and underlay the development of airway remodeling (Table 2). WBC, NEU, NLR, CRP, PCT and D-dimer were increased in blood of COPD patients. Meanwhile, serum TGF-β, SP-A, SP-D, and MMP-2/9/12 were elevated in COPD, suggesting co-existence of reactive alveolar destruction and tissue repair.

Assessment of Blood TGF-β and Abhd2 on the Severity of COPD

In COPD, TGF-β was elevated in blood but not in BALF (Table 2). A multiple logistic regression equation was constructed for the risk of COPD, and the results showed that serum TGF-β had a statistically significant effect on the risk of COPD (OR = 1.184, 95% CI 1.014–1.382, $P = 0.032$); TGF-β in BALF had no statistically significant effect on the risk of COPD ($P > 0.05$). Correlation analysis showed that serum TGF-β was negatively correlated with multiple pulmonary function parameters ($P < 0.05$). The worse the pulmonary function, the higher the serum TGF-β index (Figure 3A). The expression of Abhd2 protein in blood monocytes of COPD patients decreased (Figure 3B and C) and was negatively correlated with serum TGF-β, suggesting a protective effect of Abhd2 (Figure 3D).

Patients with COPD were divided into two groups according to prognosis, with Group B having more episodes, worse pulmonary function, and higher dyspnea index score (mMRC and CAT), as shown in Table 3. In Group B, Abhd2 protein expression and FEV1% pred decreased (Figure 3E and F), but TGF-β, SP-A, SP-D and MMP-2/9/12 in blood increased significantly, which suggested the ability of Abhd2 protein to respond to alveolar secretory function impairment and inflammatory status in COPD ($P < 0.05$). Similarly, there was no significant difference in TGF-β in BALF within groups ($P > 0.05$).

Table 2 Laboratory Inflammatory Indicators

Groups		Overall (n = 119)	COPD (n = 89)	Control (n = 30)	P Value
Laboratory inflammatory findings	**Serum TGF-β (pg/mL)**	53.01 (45.69, 73.49)	61.16 (49.93, 76.38)	45.54 (44.67, 48.15)	**<0.001**
	BAL TGF-β (pg/mL)	47.95 ± 6.81	47.69 ± 6.82	48.48 ± 7.12	0.770
	Serum-SP-A (ng/mL)	31.09 (16.14, 52.44)	44.16 (26.69, 67.23)	22.57 (6.03, 33.69)	<0.001
	Serum-SP-D (ng/mL)	83.79 (27.58, 121.95)	78.66 (46.28, 109.79)	66.16 (42.59, 77.36)	0.031
	MMP-2 (ng/mL)	31.53 (31.44, 31.58)	31.45 (31.40, 31.55)	31.41 (31.33, 31.44)	<0.001
	MMP-9 (ng/mL)	33.10 (31.10, 39.61)	33.81 (30.95, 39.11)	29.65 (24.56, 33.98)	0.001
	MMP-12 (ng/mL)	5.71 (5.22, 6.35)	5.74 (5.28, 6.44)	5.24 (4.71, 5.56)	0.001
Routine blood tests	**White blood cell count (10^9/L)**	7.59 ± 2.35	8.00 ± 2.56	6.35 ± 0.67	<0.001
	Neutrophil count (10^9/L)	5.03 ± 2.04	5.43 ± 2.14	3.82 ± 1.02	<0.001
	Lymphocyte count (10^9/L)	1.53 (1.07, 2.11)	1.58 (1.00, 2.25)	1.78 (1.09, 2.12)	0.651
	NLR	2.79 (1.80, 5.07)	3.04 (2.07, 5.63)	2.39 (1.61, 3.69)	0.006
	Eosinophil count (10^9/L)	0.10 (0.05, 0.20)	0.12 (0.06, 0.26)	0.09 (0.05, 0.26)	0.743
	Platelet count (10^9/L)	217.50 (190.50, 286.50)	231.00 (200.50, 281.50)	239.00 (194.00, 292.50)	0.971
	CRP (mg/L)	5.61 (2.25, 35.08)	7.79 (3.13, 28.20)	2.22 (1.72, 3.25)	<0.001
	PCT (μg/L)	0.19 (0.19, 0.93)	0.53 (0.18, 0.92)	0.19 (0.05, 0.19)	<0.001
	D-Dimer (mg/L)	0.33 (0.23, 0.87)	0.51 (0.28, 1.40)	0.25 (0.14, 0.40)	<0.001

Note: Data were shown as mean ± SD and Median (P25, P75). Bold font indicated emphasis.

Abbreviations: BALF, bronchoalveolar lavage fluid; COPD, chronic obstructive pulmonary disease; CRP, C-reactive protein; MMP, matrix metalloproteinase; NLR, Neutrophil to lymphocyte ratio; PCT, procalcitonin; SP-A, surfactant protein A; SP-D, surfactant protein D.

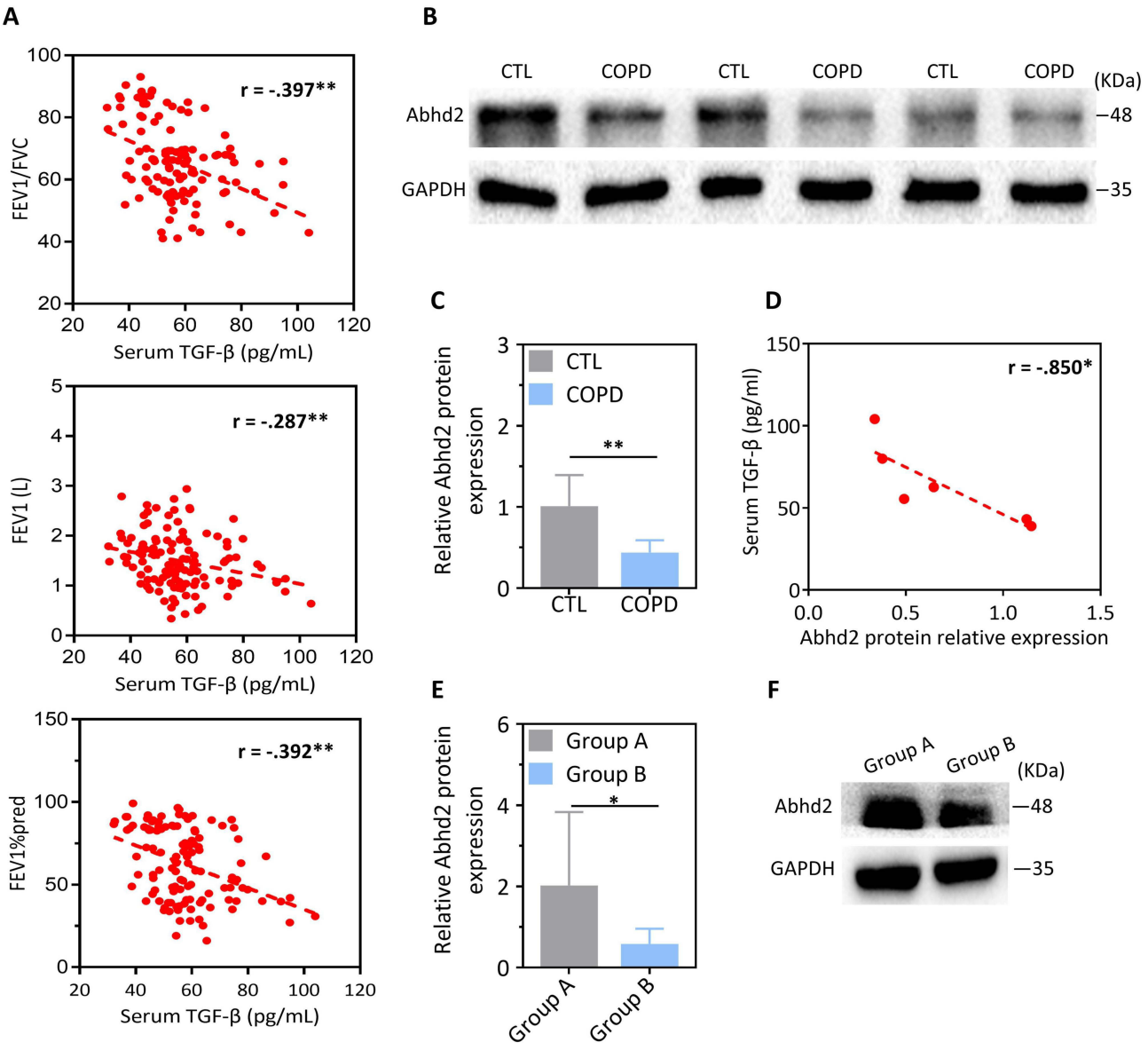

Figure 3 Clinical Abhd2 expression and airway remodeling indicators in COPD. (**A**) Correlation analysis between serum TGF-β and pulmonary function by Spearman in all participants. (**B** and **C**) Reduced Abhd2 protein expression in blood monocytes of COPD patients detected by Western blot. (**D**) Serum TGF-β negatively correlated with Abhd2 relative expression using the Pearson test. (**E** and **F**) Comparison of Abhd2 protein expression detected by Western blot within COPD groups. *$P < 0.05$, **$P < 0.01$.

Animal Genetic Identification

Agarose gel electrophoresis for identification of DNA. The results showed that the DNA band was clear under UV lamp irradiation (Figure 4A). *Abhd2*$^{Gt/Gt}$ was the desired homozygous mutant mouse when primer set G1-G2 (663 bp fragment) was met as negative and primer set G2-G3 (425 bp fragment) was positive. Wild type mice were defined as positive for primer set G1-G2 and negative for primer set G2-G3. Heterozygous mice were identified when both primer sets were positive. Quantitative real-time PCR results showed that the relative *Abhd2* mRNA expression was reduced in *Abhd2*$^{Gt/Gt}$ mice (Figure 4B). Western blot result with reduced Abhd2 protein expression confirmed successful gene knockout in *Abhd2*$^{Gt/Gt}$ mice, which was consistent with the above (Figure 4C and D).

Assessment of General Condition and Airway Remodeling in Mice

Abhd2 gene deletion affected mouse growth and development. All mice were 6–7 months old after periodic stimulation and showed abnormalities in appearance and behavior, with dim hair, alopecia, bradykinesia, and weight loss. The weight

Table 3 Indicators for COPD Patients Regrouped According to Prognosis

Groups	Overall (n = 89)	Group A (n = 41)	Group B (n = 48)	T	P value
Age (Years)	63.47 ± 9.92	60.58 ± 9.95	65.93 ± 9.24	2.629	0.010
Smoking index	392.13 ± 502.91	217.07 ± 335.90	541.67 ± 572.68	3.316	0.001
FEV1% pred (%)	54.01 ± 19.58	71.57 ± 12.82	39.01 ± 8.87	−13.697	<0.001
Serum TGF-β (pg/mL)	63.04 ± 27.41	57.05 ± 10.06	68.16 ± 35.53	2.070	**0.043**
BAL TGF-β (pg/mL)	47.69 ± 6.82	48.57 ± 4.91	47.10 ± 8.00	−0.463	0.649
Abhd2 protein relative expression	1.30 ± 1.43	2.02 ±1.81	0.58 ± 0.37	2.342	**0.045**
SP-A (ng/mL)	51.62 ± 32.93	41.67 ± 27.04	60.13 ± 35.32	2.789	0.007
SP-D (ng/mL)	85.11 ± 52.82	68.51 ± 33.98	99.29 ± 61.61	2.972	0.004
MMP-2 (ng/mL)	31.48 ± 0.14	31.41 ± 0.08	31.54 ± 0.16	4.888	<0.001
MMP-9 (ng/mL)	37.20 ± 18.88	31.31 ± 4.13	42.24 ± 24.43	3.048	0.004
MMP-12 (ng/mL)	6.34 ± 4.16	5.29 ± 0.90	7.23 ± 5.48	2.247	0.027
CAT	23.92 ± 3.67	23.05 ± 3.22	24.67 ± 3.90	2.110	0.038
mMRC	2.39 ± 0.75	2.07 ± 0.69	2.67 ± 0.69	4.043	<0.001
PaCO2 (mmHg)	41.21 ± 11.67	40.10 ± 12.34	42.17 ± 11.10	0.831	0.408
PaO2 (mmHg)	75.08 ± 14.01	79.51 ± 12.69	71.29 ± 14.09	−2.869	0.005

Note: Data were shown as mean ± SD. Bold font indicated emphasis.
Abbreviations: BALF, bronchoalveolar lavage fluid; CAT, COPD assessment test; MMP, matrix metalloproteinase; mMRC, modified Medical Research Council; SP-A, surfactant protein A; SP-D, surfactant protein D.

of mice was weighed before each CSE stimulation and found to increase over time. However, *Abhd2*$^{Gt/Gt}$ mice used for COPD model construction had increased mortality and markedly slower weight gain, especially on the 44th day (Figure 4E-G, Table S3). Chronic CSE combined with LPS stimulation damages airway structures and lung parenchyma. Wild type mice had neatly arranged airway epithelium, inconspicuous inflammatory cells, and intact alveolar structures. Compared with the WT group, the other four groups of mice showed different degrees of ciliated cell detachment, alveolar wall destruction, inflammatory cell infiltration, submucosal gland hyperplasia, smooth muscle thickening, and increased collagen fibers (HE and Masson), as shown in Figure 4H-K. What's more, *Abhd2*$^{Gt/Gt}$ promoted CSE-induced airway remodeling. Among them, the highest MLI and collagen volume ratio appeared in the ABSM group, which could be altered after treatment with a TGF-β inhibitor (SB-431542) (Figure 4L and M).

Abhd2 Deletion Aggravated Alveolar Injury via TGF-β

Absence of *Abhd2* led to elevated TGF-β and abnormal pulmonary surfactant secretion. Abhd2 protein in lung tissue decreased in WTSM group. And immunohistochemical results showed increased TGF-β positivity in lung sections after LPS-CSE stimulation or *Abhd2*$^{Gt/Gt}$ (66.7 vs 46.7 vs 93.3 vs 20.0, $P < 0.05$), especially in the ABSM group. Moreover, the addition of the drug SB-431542 suppressed TGF-β transcription and expression (Figure 5A, Table 4).

As for SPs, the positive rates of SP-A (40.0 vs 60.0) or SP-D (46.7 vs 73.3) in lung tissue sections of mice were decreased in the ABSM group compared with those in the WTSM group. Interestingly, mice treated with TGF-β inhibitors showed the opposite trend in the ABSMSB group (Figure 5B and C, Table 4). SP-A/C/D in peripheral blood was increased by ELISA after CSE stimulation, especially in ABSM group by post-hoc multiple comparisons ($P < 0.05$). Similarly, its expression decreased after addition of TGF-β inhibitors. LPS-CSE stimulation or *Abhd2*$^{Gt/Gt}$ or both decreased SPs expression in BAL, especially in the ABSM group, which was lowest and higher than that in the ABSMSB group ($P < 0.05$) (Figure 5D - F). Western blot was

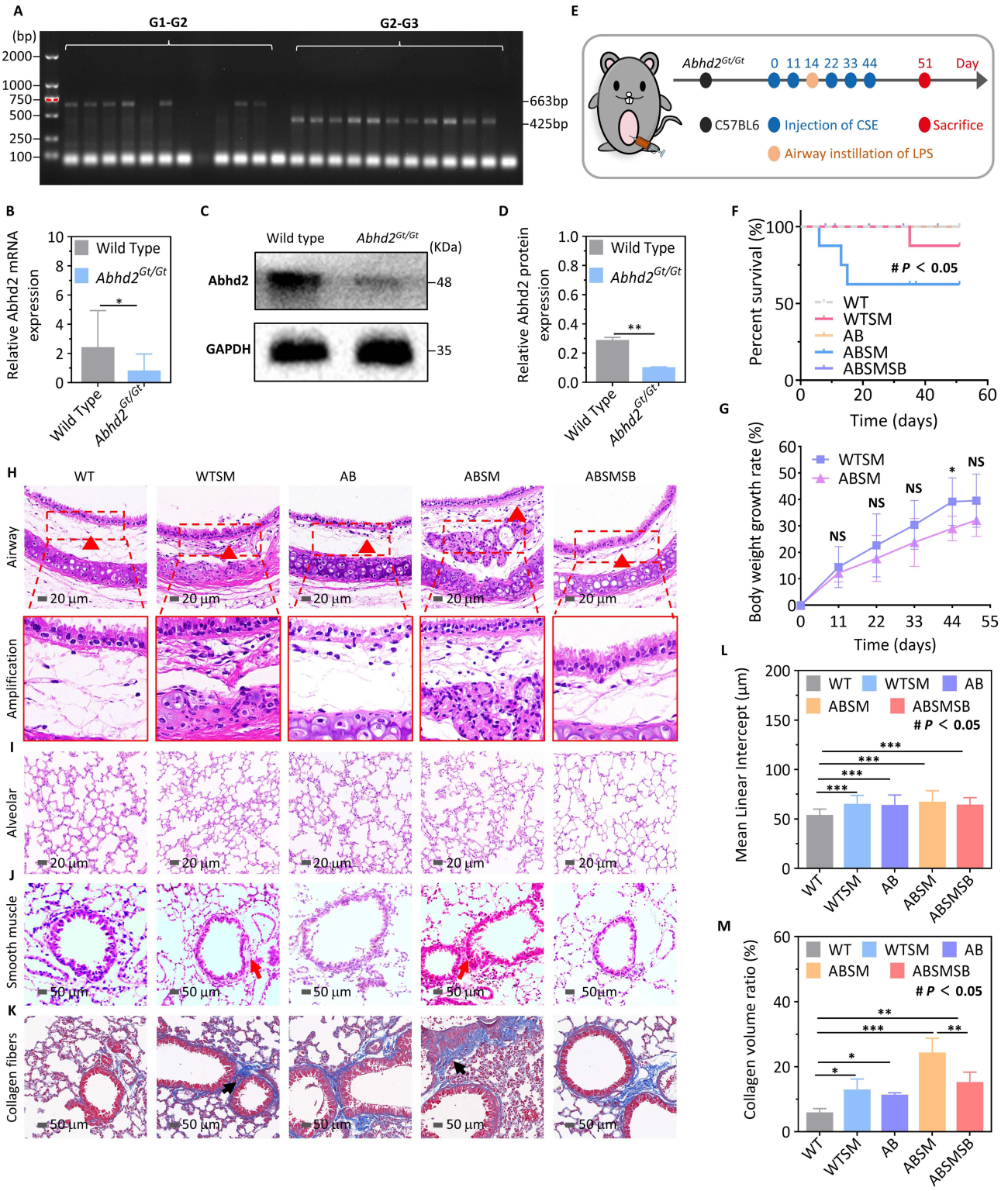

Figure 4 Gene identification and pathological observation of respiratory tract in mice. (**A**) DNA agarose gel electrophoresis results of mice. Mice were identified with primer sets G1-G2 (663 bp fragment) and primer sets G2-G3 (425 bp fragment): –/+, homozygous mutant mice (*Abhd2*$^{Gt/Gt}$); + /+, heterozygous mice; + / –, wild type mice. (**B**) Relative expression of Abhd2 mRNA in lung tissue. (**C** and **D**) Expression of Abhd2 protein in lung tissue detected by Western blot. (**E**) Flow Chart of Mouse Model Construction. (**F**) Survival curve of different groups. (**G**) Body weight growth trend of COPD mice. (**H**) Changes of airway epithelium, glands, and inflammatory cells (HE×400). Red triangles pointed to inflammatory cells. (**I**) Representative pictures of alveolar spaces and alveolar walls (HE×400). (**J**) Observation of smooth muscle thickness in lung (HE×200). Red arrows were thickened smooth muscle. (**K**) Collagen fibers stained with Masson (Magnification, ×200). Black arrows pointed to collagen fibers stained blue. (**L**) Comparison of mean lining intervals (MLI) in mouse lung tissue. (**M**) Comparison of collagen volume ratio calculation among groups. Multiple group comparisons were performed by ANOVA analysis and post hoc multiple comparisons were performed by Bonferroni method. *P < 0.05; **P < 0.01; ***P < 0.001; # P < 0.05, comparison of overall means among five groups (ANOVA); NS, not significant.

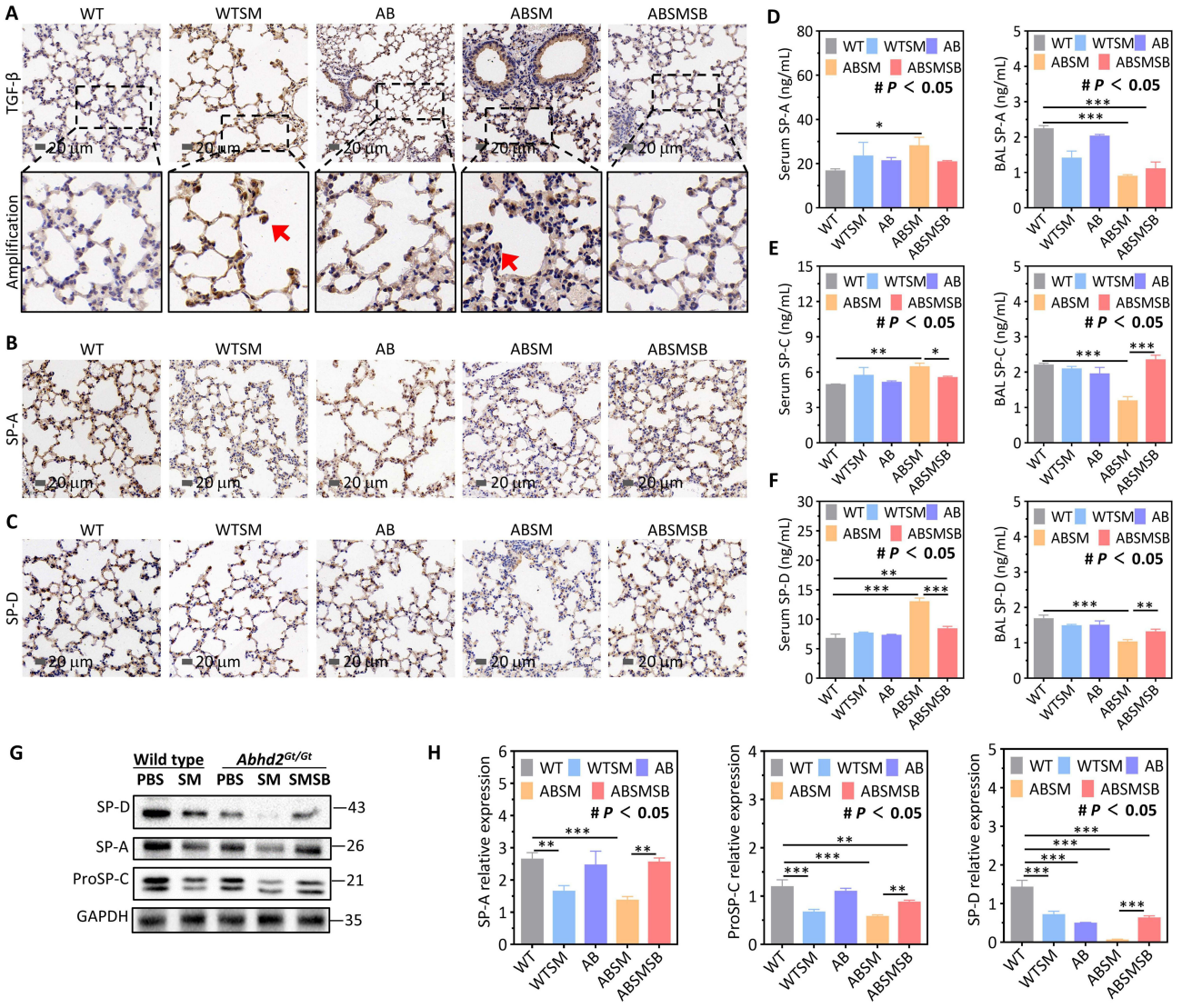

Figure 5 TGF-β expression and alveolar secretory function injury in lung. (**A**) Abhd2 deletion and CSE stimulation promoted TGF-β expression in lung tissue detected by immunohistochemistry (Magnification, ×400). Red arrows pointed to inflammatory factor distribution. (**B**) Staining observation of SP-A secreted in lung detected by immunohistochemistry (Magnification, ×400). (**C**) Staining observation of SP-D secreted in lung detected by immunohistochemistry (Magnification, ×400). (**D**) Expression of SP-A in peripheral blood and BALF of five groups of mice detected by ELISA. (**E**) Expression of SP-C in peripheral blood and BALF of five groups of mice detected by ELISA. (**F**) Expression of SP-D in peripheral blood and BALF of five groups of mice detected by ELISA. (**G** and **H**) Expression of pulmonary surfactant proteins in mouse lung homogenates detected by Western blot. Multiple group comparisons were performed by ANOVA analysis and post hoc multiple comparisons were performed by Bonferroni method. *P < 0.05; **P < 0.01; ***P < 0.001; # P < 0.05, comparison of overall means among five groups (ANOVA).

used to detect SPs in mouse lung tissue, and their expression decreased to varying degrees after CSE stimulation, which could be changed by the addition of TGF-β inhibitors ($P < 0.05$) (Figure 5G and H).

Abhd2 depletion affected alveolar cell numbers (Figure 6A-D). Alveolar cell injury was detected by counting the number of AECII stained with anti-ProSP-C antibody (Figure 6B and D) and macrophages labeled with anti-F4/80 antibody (Figure 6A and C) within 1000 cells, and the results showed differences in the overall mean number of the five groups (ANOVA, $P < 0.05$). Compared with WT group, the infiltration of macrophages increased and the number of AECII decreased in *Abhd2*$^{Gt/Gt}$ mice and LPS-CSE treated mice by post hoc multiple comparison, especially in ABSM group ($P < 0.05$). After treatment with TGF-β inhibitors, alveolar macrophage decreased ($P < 0.05$) and AECII increased.

Similarly, inflammatory factors in lung tissue showed the same trend (Figure 7A-F). ANOVA analysis showed that mRNA expression of several inflammatory factors, including IL-1α, IL-1β, IL-8, NF-κB, TGF-β, and TNF-α, was increased in the other four groups compared with the WT group, especially in ABSM group ($P < 0.05$). Treatment with TGF-β inhibitors

Table 4 Positive Expression Rate of Immunohistochemical Section

Groups	n	TGF-β	SP-A	SP-D
		Positive% (n)	Positive% (n)	Positive% (n)
WT	15	33.3 (5)	100.0 (15)	100.0 (15)
WTSM	15	66.7 (10)	60.0 (9)	73.3 (11)
AB	15	46.7 (7)	80.0 (12)	80.0 (12)
ABSM	15	93.3 (14)	40.0 (6)	46.7 (7)
ABSMSB	15	20.0 (3)	73.3 (11)	66.7 (10)
χ2	/	19.979	15.145	12.176
P value		0.001	0.003	0.014

Note: Data were analyzed by Chi-square test and presented as percentages.

altered the expression of inflammatory factors induced by LPS-CSE stimulation promoted by *Abhd2* depletion. In addition, peripheral blood differential counts analyzed by Bayer ADVIA2120 showed statistically significant differences in neutrophils, lymphocytes, as well as NLR among the five groups of mice ($P < 0.05$) (Figure 7G-N). In the peripheral blood of emphysema model mice constructed by LPS-CSE or $Abhd2^{Gt/Gt}$, neutrophils increased and lymphocytes decreased. Moreover, $Abhd2^{Gt/Gt}$ promoted an increase in neutrophil count and percentage calculation (WT vs AB; WTSM vs ABSM), which could be suppressed by TGF-β inhibitor treatment.

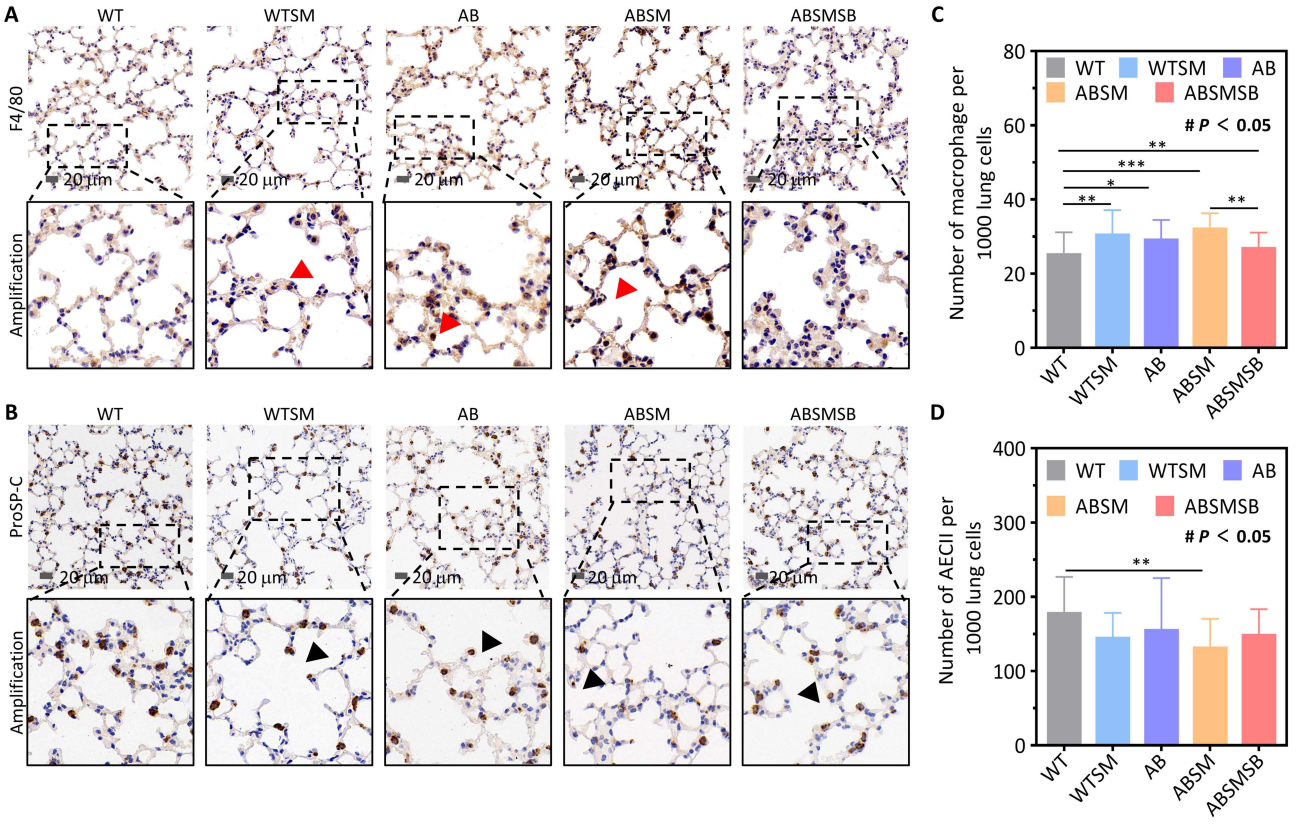

Figure 6 Observation of alveolar cell injury in mice by immunohistochemistry. (**A** and **C**) Macrophages were labeled with anti-F4/80 antibody and counted with ImageJ software (Magnification, ×400). (**B** and **D**) Alveolar type II cells were labeled with specific anti-ProSP-C antibody and counted with ImageJ software (Magnification, ×400). Red triangles referred to stained macrophages and black triangles pointed to stained alveolar type II cells. Multiple group comparisons were performed by ANOVA analysis and post hoc multiple comparisons were performed by Bonferroni method. *$P < 0.05$; **$P < 0.01$; ***$P < 0.001$; # $P < 0.05$, comparison of overall means among five groups (ANOVA).

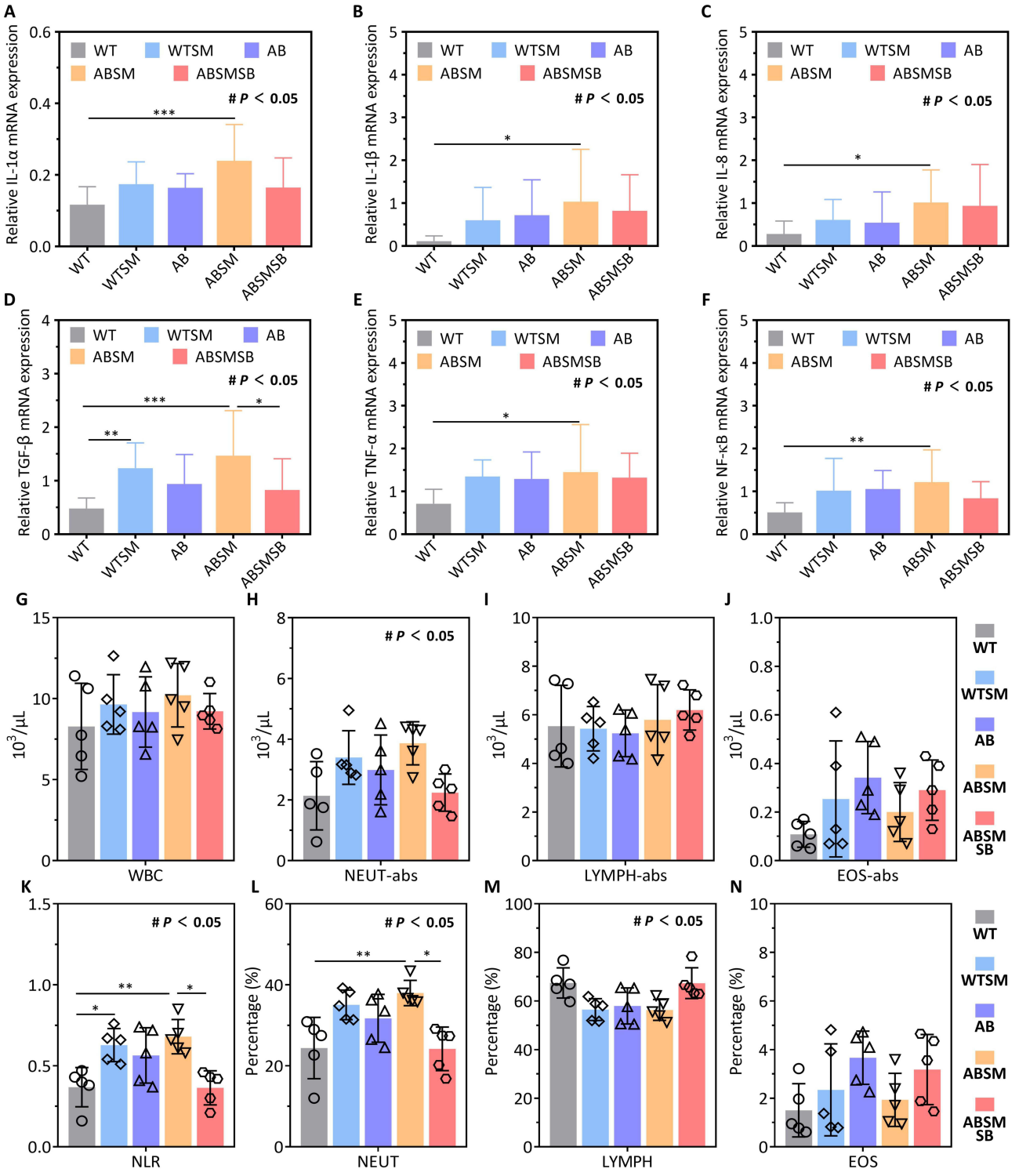

Figure 7 Inflammatory factors mRNA expression in lung tissue detected by RT-PCR and hematological data for differential cell counts and percentages in mice. (**A**) *Abhd2*$^{Gt/Gt}$ promoted the relative expression of IL-1α mRNA in lung. (**B**) *Abhd2*$^{Gt/Gt}$ promoted the relative expression of IL-1β mRNA in lung. (**C**) *Abhd2*$^{Gt/Gt}$ promoted the relative expression of IL-8 mRNA in lung. (**D**) The relative expression of TGF-β mRNA in lung of five groups. (**E**) *Abhd2*$^{Gt/Gt}$ promoted the relative expression of TNF-α mRNA in lung. (**F**) *Abhd2*$^{Gt/Gt}$ promoted the relative expression of NF-κB mRNA in lung. (**G**) White blood cell count. (**H**) Neutrophil count. (**I**) Lymphocyte count. (**J**) Eosinophil count. (**K**) Neutrophil to lymphocyte ratio. (**L**) Percentage of neutrophils in total leukocytes. (**M**) Percentage of lymphocytes in total leukocytes. (**N**) Percentage of eosinophils in total leukocytes. Multiple group comparisons were performed by ANOVA analysis and post hoc multiple comparisons were performed by Bonferroni method. **P* < 0.05; ***P* < 0.01; ****P* < 0.001; # *P* < 0.05, comparison of overall means among five groups (ANOVA).

https://doi.org/10.2147/COPD.S440200 DovePress

TGF-β Inhibitors Attenuated EMT Aggravated by Abhd2 Depletion

Immunofluorescence and Western blot were performed on mouse lung tissue to detect the process of EMT, including E-cadherin labeling of airway epithelium, ZO1 labeling of tight junctions between cells and vimentin labeling of mesenchyme (Figure 8A-D). The immunofluorescence results showed that the expression of E-cadherin and ZO1 decreased and vimentin increased in lung tissue of *Abhd2*$^{Gt/Gt}$ mice and LPS-CSE treated mice compared with WT

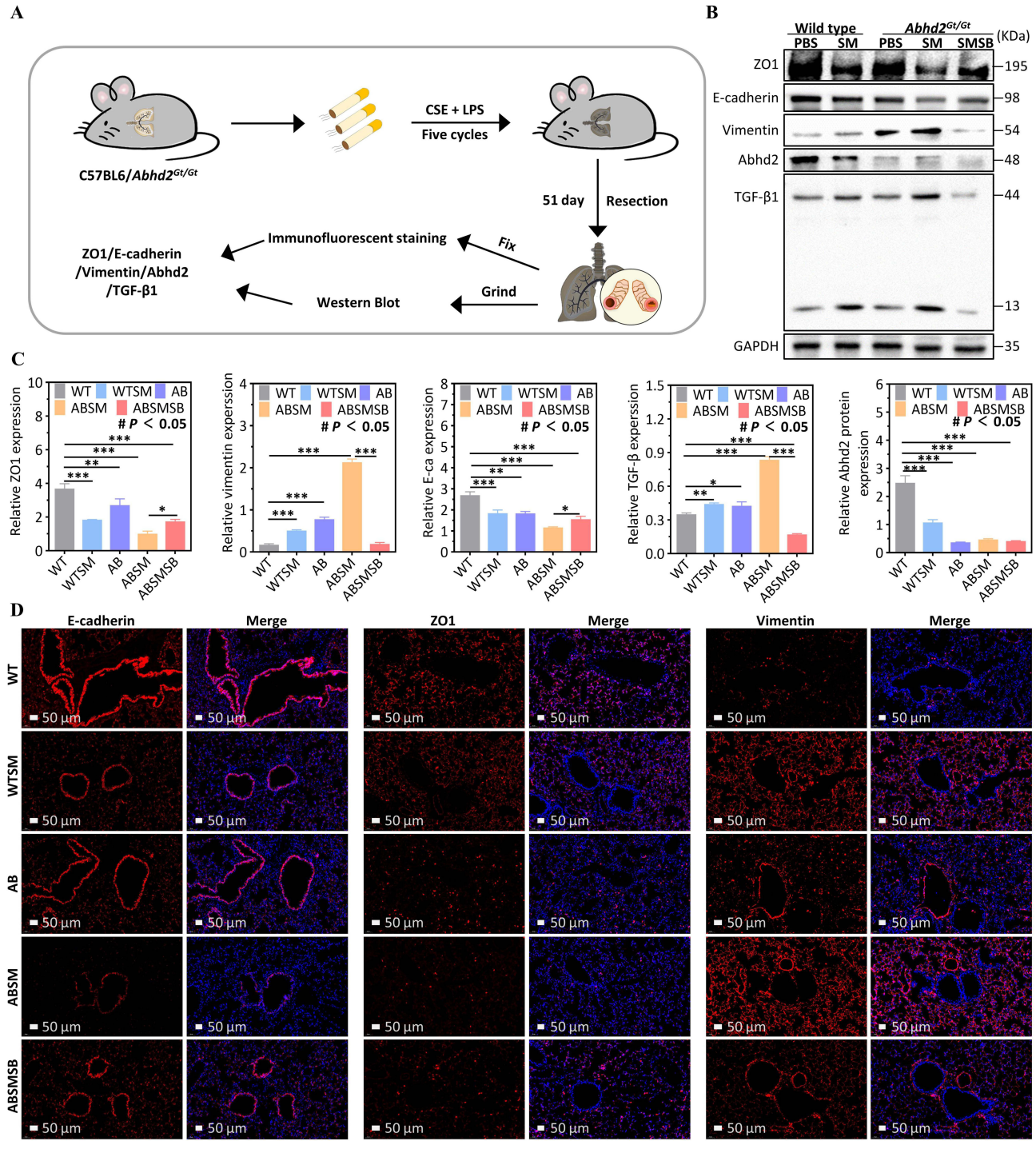

Figure 8 Detection of EMT markers in mouse lung. (**A**) Origin of mouse tissues. (**B** and **C**) Expression of TGF-β, E-cadherin, ZO-1 and Vimentin detected by Western blot. (**D**) Expression of E-cadherin, ZO-1 and Vimentin in lung tissue detected by immunofluorescence (Magnification, ×200). Multiple group comparisons were performed by ANOVA analysis and post hoc multiple comparisons were performed by Bonferroni method. *$P < 0.05$; **$P < 0.01$; ***$P < 0.001$; # $P < 0.05$, comparison of overall means among five groups (ANOVA).

group, especially ABSM group. Compared with ABSM mice, ABSMT mice had increased E-cadherin and ZO1 but decreased vimentin expression. And Western blot results supported the above trends (Figure 8B and C).

Discussion

The mortality rate of COPD ranks in the top three in the world and has aroused the attention and research of many researchers.[22] In particular, *Abhd2* has been considered a susceptibility gene for the pathogenesis of COPD, but the mechanism is still limited and rarely studied. Recently, the involvement of TGF-β in inflammation-mediated COPD and fibrotic lesions by regulating tissue repair as well as receptor expression and function of immune cells is a research hotspot. In previous work, our team identified abnormal mRNA expression of TGF-β in lung tissue of *Abhd2*$^{Gt/Gt}$ mice, which underlies this subject.[15] In this study, we demonstrated for the first time that *Abhd2* down-regulation promoted COPD progression induced by CSE combined with LPS in association with TGF-β, and the findings of altered airway remodeling were presented below.

Firstly, we considered that Abhd2 protein could exert a protective effect in the lung, which might be damaged by cigarettes. Abhd2, a member of the Abhd protein family, has been identified as a lipase and found to be expressed on AECII and macrophage. However, its biological mechanism is still unclear. In previous clinical studies, we have found that rs 12442260 polymorphism in *Abhd2* gene was associated with the risk of COPD.[23] In this study, we demonstrated for the first time that Abhd2 protein expression was decreased in peripheral blood mononuclear cells of COPD patients, especially in people with poor pulmonary function, which suggested a protective effect of Abhd2 on the lung and a guiding significance for the prognosis of COPD. At the same time, we found that both the Group B population with worse prognosis who preferred smoking and the COPD model mice constructed by CSE were accompanied by more severe Abhd2 protein reduction, suggesting that cigarettes may be one of the irritating factors for Abhd2 depletion or decreased secretion. According to statistics, 50% of smokers suffer from COPD due to ROS activation, enhanced EMT and AKT signaling, and increased TGF-β.[24] Harmful components of cigarettes can influence genetic susceptibility by inducing DNA damage, epithelial cell reprogramming, transcription factor deregulation and mitochondrial dysfunction, which may be associated with a decrease in *Abhd2* and need to be further confirmed in the future.[25]

Secondly, this study confirmed the role of *Abhd2* in the pathogenesis of COPD. Airway remodeling, as a typical feature of COPD pathology, is influenced by both chronic inflammatory stimuli and genetic factors. Genetically, Jin's team found that 6-month-old *Abhd2*$^{Gt/Gt}$ mice spontaneously developed emphysema models,[15] which was also a reference for our animal selection. This study found that the reduction of *Abhd2* in COPD patients or deletion in transgenic mice promoted airway remodeling in COPD, especially in the presence of cigarette factors. In animals, downregulation of *Abhd2* inhibited AECII expression and SPs secretion in COPD, promoted severe destruction of the alveolar wall, thickening of collagen fibers and smooth muscle, secretion of inflammatory factors, macrophage infiltration, and EMT progression. In clinical study, we found that the expression of several inflammatory factors such as CRP, MMPs, SPs, and TGF-β was increased in COPD patients, which was consistent with previous studies.[26] MMPs are capable of degrading multiple components of the extracellular matrix and are involved in cell growth, differentiation, and repair. At the same time, SPs can be combined with macrophages to increase phagocytosis of pathogens in immunomodulatory and inflammatory responses in the lung. Therefore, the decreased Abhd2 protein and abnormal expression of multiple inflammatory factors in COPD suggested that alveolar destruction coexists with airway repair after tissue injury, confirming that the effect of inflammatory mechanisms on airway remodeling was tightly linked to genetics.

Thirdly, TGF-β could be a key factor in *Abhd2* regulation of airway remodeling in COPD. TGF-β is a key factor in maintaining normal function of cells and is involved in the regulation of immune homeostasis as well as the development of inflammatory diseases. Previous studies have confirmed that TGF-β expression was increased on bronchial epithelial cells in COPD, and could increase the incidence of lung tumors and pulmonary fibrosis.[27–30] In humans, the results of this study showed that serum TGF-β was closely related to the expression of *Abhd2* in monocytes and pulmonary function parameters of FEV1/FVC, FEV1, and FEV1% PRED, indicating the predictive significance for COPD progression. In animals, *Abhd2*$^{Gt/Gt}$ mice developed elevated TGF-β secretion and airway remodeling, and the above pathological phenomena were more significant under LPS-CSE stimulation but inhibited after blocking TGF-β

expression. In COPD, increased macrophage expression as immune cells can exacerbate mucosal injury by affecting their function of phagocytosis and antigen presentation, and secretion of inflammatory factors. Notably, TGF-β not only acts as a regulator of macrophage polarization, but also participates in ECM remodeling by regulating the secretion of collagen fibers, MMPs. The occurrence of EMT, characterized by loss of adhesion and polarity between cells, is a risk warning for poor prognosis in COPD and a potential factor for concurrent lung cancer. Most importantly, TGF-β is one of the key cores in these multiple signaling pathways. *Abhd2* as a unique class of lipase could regulate triglyceride metabolism. In lipid metabolism, TGF-β can facilitate triglyceride deposition due to free fatty acid activation, sphingomyelin synthase reduction, and choline kinase overexpression. This is also the possible reason why alveolar epithelial cells could not be completely repaired in this study due to the coexistence of multiple factors despite the addition of TGF-β inhibitors in the ABSMSB group (Figure 4L). Obviously, these confirmed the involvement of TGF-β in *Abhd2*-regulated COPD signal transduction pathways. In COPD, the combination of acute exacerbation of chronic inflammation and genetic factors, jointly promotes tissue destruction and repeated incomplete repair, leading to airway structural changes and airway remodeling. However, cells capable of secreting TGF-β and expressing *Abhd2* are not unique, such as macrophages and AECII. Although we have tried to extract primary cells from transgenic mice to deeply investigate the mechanism, it failed due to low survival rate, which is also a limitation of this study. Fortunately, in ongoing cell pre-experiments, we successfully constructed an *Abhd2* silencing model of A549 cells with AECII features, and initially found lipid deposition and ROS activation (Figure S1 and Figure S2), which further validated the essential features of *Abhd2*. Next, we will deeply excavate what are the key molecules of *Abhd2* regulating TGF-β.

Additionally, another important implication of our work was that *Abhd2* could be related to body growth and metabolism. In this study, we found that $Abhd2^{Gt/Gt}$ mice gained weight slowly compared with healthy mice, and the deletion of *Abhd2* could aggravate the imbalance of body mass in COPD model mice induced by CSE combined with LPS ($P < 0.05$). However, no differences in body weight were found in clinical studies, which could be associated with uncontrollable human dietary habits. *Abhd2* deletion not only activates the release of inflammatory cells and pro-inflammatory mediators, but also leads to metabolic abnormalities as it is essentially a lipase whose downregulation leads to lipid accumulation. Besides, we had tried to construct COPD models more realistically by inhaling smoke,[19] but failed due to high sensitivity to external stimuli and high mortality of $Abhd2^{Gt/Gt}$ mice, which was why our model protocol was modified and new ideas needed to be continuously tried and explored. In the future, we can conduct further studies on metabolic mechanisms from the direction of skeletal muscle atrophy.

In summary, we confirmed that *Abhd2* down-regulation easily led to airway remodeling in COPD, which was also an innovative point in this study. These effects can be manifested as AECII damage, abnormal SPs secretion, macrophage infiltration and inflammatory disturbances. Meanwhile, TGF-β could modulate *Abhd2*-deficiency-induced airway mucosal and alveolar injury as well as EMT. Hence, this finding provides potential value for the assessment and prognosis of clinical COPD conditions genetically. It is worth pondering that if the specific mechanism of how *Abhd2* regulates TGF-β can be investigated, it will be very beneficial for clinical drugs to be carried out to treat COPD patients.

Conclusion

Abhd2 plays a protective role in the lung, and its abnormal expression may increase susceptibility to COPD and poor prognosis. More precisely, the reduction of *Abhd2* promotes airway remodeling mainly through regulation involving TGF-β factor, including effects on mucosal repair, smooth muscle hyperplasia, EMT, inflammatory infiltration, and pulmonary surfactant secretion, which are more pronounced in the presence of the deleterious factor cigarette.

Data Sharing Statement

The data/documents could be obtained from corresponding author.

Ethics Approval

The authors are accountable for all aspects of the work in ensuring that questions related to the accuracy or integrity of any part of the work are appropriately investigated and resolved. This study was approved by the institutional ethic committee of the Fourth Affiliated Hospital of Harbin Medical University (2022-SCILLSC-21) and informed consent

was given by all patients. All animals were maintained and experimented in accordance with the ethical guidelines of the Guiding Principles in the Care and Use of Animals (China) and the Policy of Animal Care and Use Committee of the Fourth Affiliated Hospital of Harbin Medical University. All procedures were performed in accordance with the Declaration of Helsinki and relevant national policies.

Informed Consent

The information involved in the article has obtained all the patient's oral informed consent.

Acknowledgments

This work was supported by the National Natural Science Foundation of China (81670028), Graduate Practice Innovation Project Fund of Harbin Medical University (2018182) and 2023 Scientific Research Project of Basic Scientific Research Business Fee of Provincial Institutions of Higher Education in Heilongjiang Province.

Disclosure

All authors indicate no conflict of interest in this work.

References

1. Cai Q, Fei Y, An H-W., et al. Macrophage-instructed intracellular staphylococcus aureus killing by targeting photodynamic dimers. *ACS Appl Mater Interfac*. 2018;10(11):9197–9202. doi:10.1021/acsami.7b19056
2. Mahmood MQ, Reid D, Ward C, et al. Transforming growth factor (TGF) β(1) and Smad signalling pathways: a likely key to EMT-associated COPD pathogenesis. *Respirology*. 2017;22(1):133–140. doi:10.1111/resp.12882
3. Liu HJ, Chen G, Chen L, et al. Cytokine-induced alterations of BAMBI mediate the reciprocal regulation of human Th17/Treg cells in response to cigarette smoke extract. *Int J Mol Med*. 2018;42(6):3404–3414. doi:10.3892/ijmm.2018.3919
4. Aono Y, Ledford JG, Mukherjee S, et al. Surfactant protein-D regulates effector cell function and fibrotic lung remodeling in response to bleomycin injury. *Am J Respir Crit Care Med*. 2012;185(5):525–536. doi:10.1164/rccm.201103-0561OC
5. Watson A, Clark JMW, Clark HW. SP-A and SP-D: dual functioning immune molecules with antiviral and immunomodulatory properties. *Front Immunol*. 2020;11:622598. doi:10.3389/fimmu.2020.622598
6. Vlachaki EM, Koutsopoulos AV, Tzanakis N, et al. Altered surfactant protein-A expression in type II pneumocytes in COPD. *Chest*. 2010;137(1):37–45. doi:10.1378/chest.09-1029
7. Whitsett JA, Weaver TE, Lieberman MA, et al. Differential effects of epidermal growth factor and transforming growth factor-beta on synthesis of Mr = 35,000 surfactant-associated protein in fetal lung. *J Biol Chem*. 1987;262(16):7908–7913. doi:10.1016/S0021-9258(18)47654-5
8. Zhou L, Dey CR, Wert SE, et al. Arrested lung morphogenesis in transgenic mice bearing an SP-C-TGF-beta 1 chimeric gene. *Dev Biol*. 1996;175(2):227–238. doi:10.1006/dbio.1996.0110
9. Minoo P, Hu L, Zhu N, et al. SMAD3 prevents binding of NKX2.1 and FOXA1 to the SpB promoter through its MH1 and MH2 domains. *Nucleic Acids Res*. 2008;36(1):179–188. doi:10.1093/nar/gkm871
10. Maniscalco WM, Sinkin RA, Watkins RH, et al. Transforming growth factor-beta 1 modulates type II cell fibronectin and surfactant protein C expression. *Am J Physiol*. 1994;267(5 Pt 1):L569–77. doi:10.1152/ajplung.1994.267.5.L569
11. Hsieh HL, Wang HH, Wu WB, et al. Transforming growth factor-β1 induces matrix metalloproteinase-9 and cell migration in astrocytes: roles of ROS-dependent ERK- and JNK-NF-κB pathways. *J Neuroinflammation*. 2010;7(1):88. doi:10.1186/1742-2094-7-88
12. Edgar AJJMP, Polak JM. Cloning and tissue distribution of three murine alpha/beta hydrolase fold protein cDNAs. *Biochem Biophys Res Commun*. 2002;292(3):617–625. doi:10.1006/bbrc.2002.6692
13. Lord CC, Brown GTM, Brown JM. Mammalian alpha beta hydrolase domain (ABHD) proteins: lipid metabolizing enzymes at the interface of cell signaling and energy metabolism. *Biochim Biophys Acta*. 2013;1831(4):792–802. doi:10.1016/j.bbalip.2013.01.002
14. Miyata K, Oike Y, Hoshii T, et al. Increase of smooth muscle cell migration and of intimal hyperplasia in mice lacking the alpha/beta hydrolase domain containing 2 gene. *Biochem Biophys Res Commun*. 2005;329(1):296–304. doi:10.1016/j.bbrc.2005.01.127
15. Jin S, Zhao G, Li Z, et al. Age-related pulmonary emphysema in mice lacking alpha/beta hydrolase domain containing 2 gene. *Biochem Biophys Res Commun*. 2009;380(2):419–424. doi:10.1016/j.bbrc.2009.01.098
16. Mirza S, Clay RD, Koslow MA, et al. COPD guidelines: a review of the 2018 gold report. *Mayo Clin Proc*. 2018;93(10):1488–1502. doi:10.1016/j.mayocp.2018.05.026
17. Caraci F, Gulisano W, Guida CA, et al. A key role for TGF-β1 in hippocampal synaptic plasticity and memory. *Sci Rep*. 2015;5:11252. doi:10.1038/srep11252
18. Ma J, Zhang L, Niu T, et al. Growth differentiation factor 11 improves neurobehavioral recovery and stimulates angiogenesis in rats subjected to cerebral ischemia/reperfusion. *Brain Res Bull*. 2018;139:38–47. doi:10.1016/j.brainresbull.2018.02.011
19. Lv MY, Qiang LX, Wang BC, et al. Complex evaluation of surfactant protein a and d as biomarkers for the severity of COPD. *Int J Chron Obstruct Pulmon Dis*. 2022;17:1537–1552. doi:10.2147/COPD.S366988
20. Lee KH, Lee J, Jeong J, et al. Cigarette smoke extract enhances neutrophil elastase-induced IL-8 production via proteinase-activated receptor-2 upregulation in human bronchial epithelial cells. *Exp Mol Med*. 2018;50(7):1–9. doi:10.1038/s12276-018-0187-x
21. Zhang J, Yi R, Qian Y, et al. Lactobacillus plantarum CQPC06 activity prevents dextran sulfate sodium-induced colitis by regulating the IL-8 pathway. *J Food Sci*. 2018;83(10):2653–2661. doi:10.1111/1750-3841.14346

22. Borg M, Thastrup T, Larsen KL, et al. Free diving-inspired breathing techniques for COPD patients: a pilot study. *Chron Respir Dis*. 2021;18:14799731211038673. doi:10.1177/14799731211038673
23. Liu L, Li X, Yuan R, et al. Associations of ABHD2 genetic variations with risks for chronic obstructive pulmonary disease in a Chinese han population. *PLoS One*. 2015;10(4):e0123929. doi:10.1371/journal.pone.0123929
24. Mathers CDDL, Loncar D. Projections of global mortality and burden of disease from 2002 to 2030. *PLoS Med*. 2006;3(11):e442. doi:10.1371/journal.pmed.0030442
25. Hirano T, Matsunaga K, Sugiura H, et al. Relationship between alveolar nitric oxide concentration in exhaled air and small airway function in COPD. *J Breath Res*. 2013;7(4):046002. doi:10.1088/1752-7155/7/4/046002
26. Prins HJ, Duijkers R, van der Valk P, et al. CRP-guided antibiotic treatment in acute exacerbations of COPD in hospital admissions. *Eur Respir J*. 2019;53(5):1802014. doi:10.1183/13993003.02014-2018
27. Tsubouchi K, Araya J, Minagawa S, et al. Azithromycin attenuates myofibroblast differentiation and lung fibrosis development through proteasomal degradation of NOX4. *Autophagy*. 2017;13(8):1420–1434. doi:10.1080/15548627.2017.1328348
28. Guo Y, Lu X, Chen Y, et al. Opposing roles of ZEB1 in the cytoplasm and nucleus control cytoskeletal assembly and YAP1 activity. *Cell Rep*. 2022;41(1):111452. doi:10.1016/j.celrep.2022.111452
29. Borzi C, Calzolari L, Ferretti AM, et al. c-Myc shuttled by tumour-derived extracellular vesicles promotes lung bronchial cell proliferation through miR-19b and miR-92a. *Cell Death Dis*. 2019;10(10):759. doi:10.1038/s41419-019-2003-5
30. Marwitz S, Ballesteros-Merino C, Jensen SM, et al. Phosphorylation of SMAD3 in immune cells predicts survival of patients with early stage non-small cell lung cancer. *J Immunother Cancer*. 2021;9(2):e001469. doi:10.1136/jitc-2020-001469